

SUSY phenomenology and inclusive searches

THORBEN SWIRSKI

Physikalisches Institut

Universität Freiburg

Hermann-Herder-Str. 3, 79104 Freiburg, Germany

September 4, 2014



Abstract

Current experimental data suggest that the Standard Model (SM) is very good in describing the nature of particles and their interaction. However, there are still many unsolved problems on the theoretical side or in astrophysics that suggest new physics beyond the SM, such as the dark matter problem or the hierarchy problem. One of the most promising extensions of the SM is Super Symmetry (SUSY). In this article we will discuss why this extension is particularly interesting from a theoretical point of view and with which problems of the SM in mind it was created. We will also discuss searches for different SUSY parametrisations and decay chains with ATLAS and CMS at CERN.

1 Why SUSY?

The SM fits the experimental data very well. However, few problems remain. Examples for such problems include the occurrence of dark matter, the hierarchy problem, the unification of forces at the Grand Unified Theory (GUT) scale. SUSY was created with these three problems in mind.

1.1 Dark matter

Astrophysicists observe that the gravitational lensing effect and rotational speeds of galaxies suggest far more mass than expected by the visible mass of the galaxy. This suggests new, still unobserved particles.

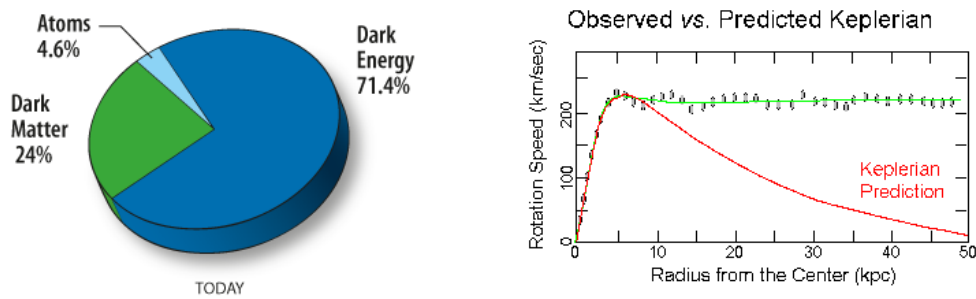


Figure 1: left - from: http://wmap.gsfc.nasa.gov/universe/uni_matter.html, right - from: <http://www.astronomy.ohio-state.edu/thompson/1144/Lecture40.html>

1.2 Hierarchy problem

The hierarchy problem can be explained at the example of the Higgs boson mass. Considering the loop correction terms of higher order, one finds contributions that are very large (diverging quadratically) that have to cancel out very precisely on many digits to allow a low Higgs boson mass of 125.5 GeV. This fine tuning is considered unnatural by many physicists and a theory that explains this is therefore favoured by many. A SUSY model with sparticle masses of around 1 TeV can give this explanation.

1.3 Unification of forces at the GUT scale

It has always been a goal to find a symmetry that can explain all forces we know in one coherent field theory. The scale at which the electromagnetic, the weak and the strong force are to be unified and therefore described in one force with one coupling constant is the so called Grand Unified Theory (GUT) scale. Extrapolating the running of the coupling strengths with today's knowledge shows that these never meet in one point. SUSY can solve this problem.

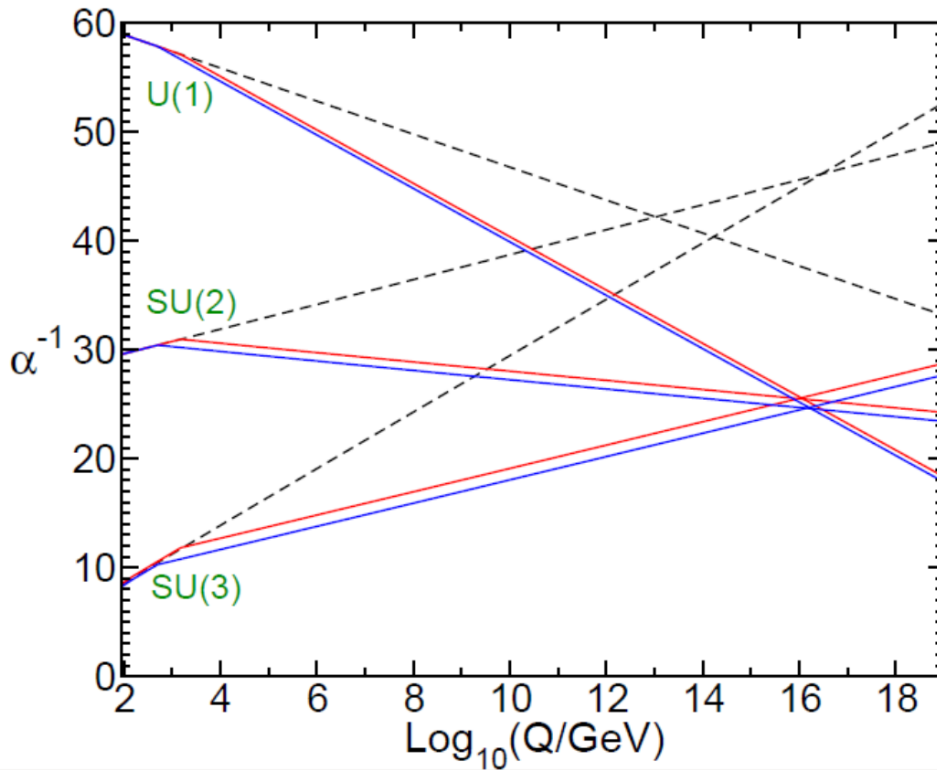


Figure 2: The evolution of the inverse coupling constants of the interactions with energy for the SM (dashed lines) and SUSY (solid lines) [1]

2 What is SUSY?

A new symmetry between fermion and boson fields can be enforced, leading to a new set of particles. With new particles, new Feynman graphs can be constructed leading to more interactions and correction terms. SUSY also requires two Higgs doublets to give all particles their masses, leading to five Higgs bosons, two of which are charged.

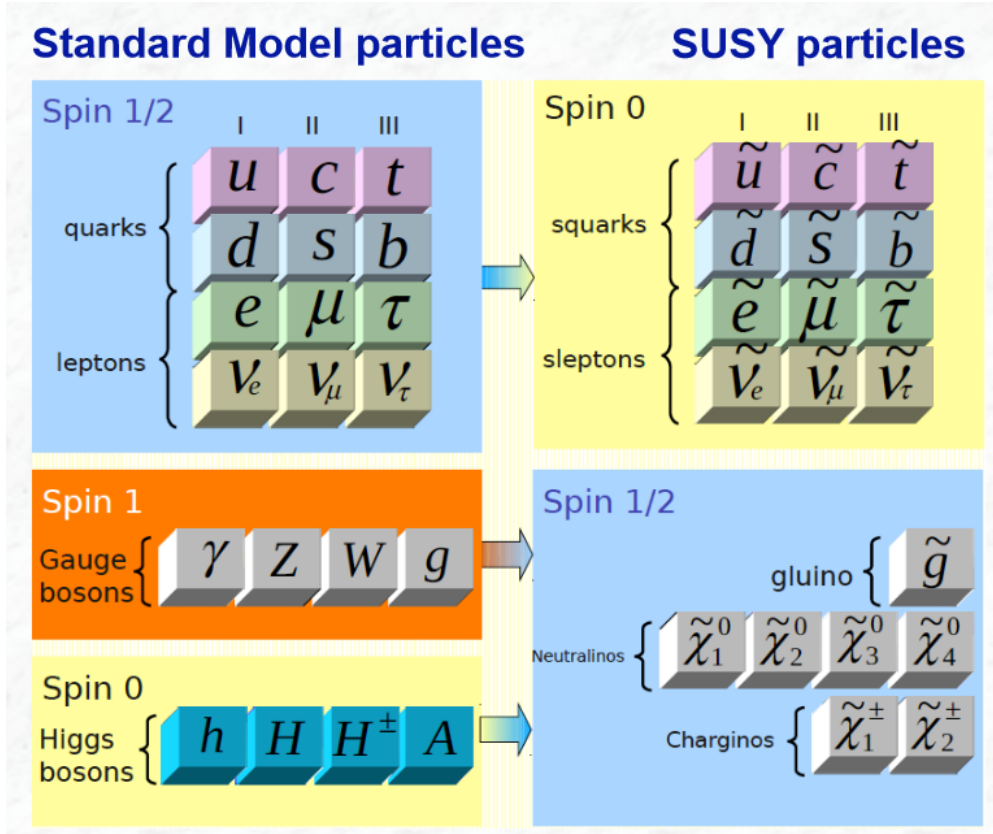


Figure 3: Particles according to SUSY [2]

The corrections for the higgs mass now cancel out quite naturally, leaving terms proportional to the mass difference between particle and sparticle. These terms remain 'natural' up to sparticle masses of 1 TeV. These new interactions, however, can lead to a proton decay which is not observed in nature. To solve this problem, a new parity is introduced. Simply enforcing this symmetry would also imply that the masses of a particle and its corresponding sparticle would be the same. Since SUSY particles have not been seen yet, the symmetry must be broken if realized in nature.

2.1 R-parity

New interactions in the SUSY sector could lead to violations of lepton and baryon numbers. Many SUSY models remedy this by introducing the so called 'R-parity':

$$R = (-1)^{3(B-L)+2S} = \begin{cases} +1 & \text{SM particle} \\ -1 & \text{SUSY particle} \end{cases}$$

Due to its multiplicative nature, R-parity conservation also implies that SUSY particles can only be produced in pairs and decay into an odd number of SUSY particles. Also, the highest SUSY particle is automatically stable.

2.2 SUSY symmetry breaking

An unbroken SUSY would imply that only the spin of the sparticle differs from the original particle. This would mean that SUSY particle should be observed at the same mass as the particle itself. Since they have not been observed, the symmetry must be broken if realised in nature. How SUSY is broken is of course not clear and the breaking can be realised in many different ways.

2.3 Minimal SUSY Standard Model (MSSM)

With the SUSY mechanism an arbitrary amount of sparticle can be created. The model of most interest is the model with the fewest particles that can be realised, the MSSM. Since the symmetry has to be broken, SUSY gauge bosons, the gauginos, mix into new mass eigenstates:

- **Charginos** $\tilde{\chi}_{1,2}^{\pm}$: mixture of charged fields \tilde{W}^{\pm} , \tilde{H}_2^{+} , \tilde{H}_1^{-}
- **Neutralinos** $\tilde{\chi}_{1,2,3,4}^0$: mixture of neutral fields \tilde{B} , \tilde{W}^3 , $\tilde{H}_{1,2}^0$

If the lightest neutralino is the lightest SUSY particle (LSP) it is a prime candidate for dark matter.

2.4 Minimal Supergravity (mSUGRA)

To localize the global symmetry of SUSY, one may introduce a spin $3/2$ field. This particle can then be interpreted as gravitino, although no gravity is implemented in the theory. Some theories keep the neutralino as LSP, some choose the gravitino.

2.5 Free parameters of the MSSM

SUSY introduces many new fields. This also leads to many new vertices, masses and other parameters. Therefore, the MSSM contains 105 free parameters, which are too many to be able to experimentally determine all of them, giving rise to the need for simplification. Most common are two different types of simplifications:

- *pMSSM*: fixing mass hierarchies of the SUSY particles to gain sensitivity to certain decay chains and topologies. This leads to 22 free parameters.
- *cMSSM*: Assumption of unification of masses at the GUT scale leads to 5 remaining parameters.

The parameters of both simplifications are listed in the following table:

Table 1: remaining free parameters of pMSSM and cMSSM

pMSSM	cMSSM
<ul style="list-style-type: none"> • sfermion masses • gaugino masses • proportionality factors of the trilinear couplings A_f • squared Higgs boson masses • $\tan \beta$ 	<ul style="list-style-type: none"> • unification of scalar masses m_0 • unification of gaugino masses $m_{1/2}$ • unification of the trilinear couplings A_0 • the sign of the higgsino mass factor μ • $\tan \beta$

Here, $\tan \beta = \frac{v_1}{v_2}$ with v_1 and v_2 being the vacuum expectation values of the Higgs field.

3 SUSY event topology

SUSY events are very diverse, reaching from pair production to multistage decay cascades. The events usually have large amounts of missing transverse energy due to the LSP escaping the detector undetected, can have multiple jets and multiple leptons.

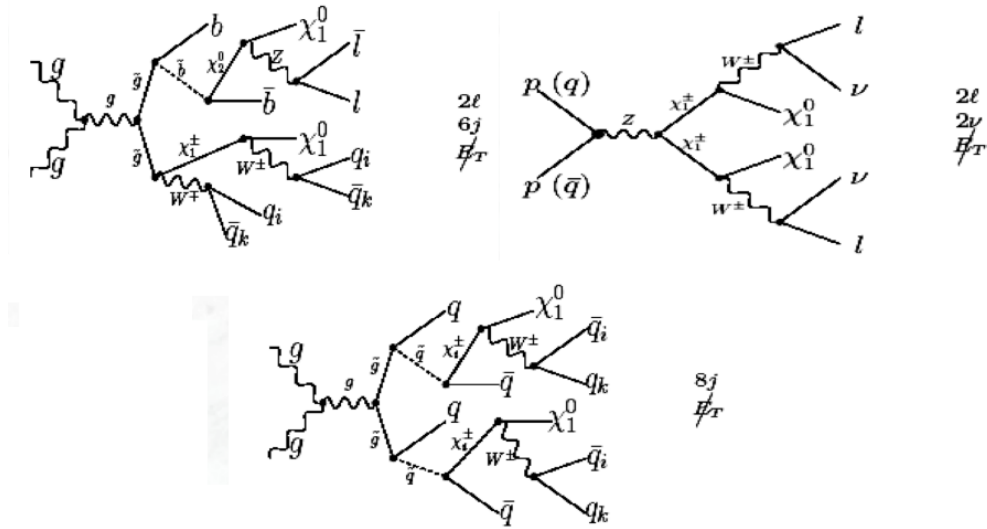


Figure 4: some examples of SUSY events [3]

4 Searches for SUSY with the LHC

Many different searches for SUSY have been performed with the LHC. They are usually divided by jet and lepton multiplicity. Three of these searches will be introduced in this chapter.

4.1 2-6 jets + 0 leptons search by ATLAS

10 different signal regions are defined in this search. Signal regions differ primarily by jet multiplicity, followed by more or less stringent cuts on the introduced variable m_{eff} , the scalar sum of the p_T of the N highest p_T jets and $m_{\text{eff}}(\text{incl.})$ which contains all jets.

Requirement	Channel									
	A (2-jets)		B (3-jets)		C (4-jets)		D (5-jets)	E (6-jets)		
	L	M	M	T	M	T	–	L	M	T
$E_T^{\text{miss}}[\text{GeV}] >$	160									
$p_T(j_1) [\text{GeV}] >$	130									
$p_T(j_2) [\text{GeV}] >$	60									
$p_T(j_3) [\text{GeV}] >$	–		60		60		60		60	
$p_T(j_4) [\text{GeV}] >$	–		–		60		60		60	
$p_T(j_5) [\text{GeV}] >$	–		–		–		60		60	
$p_T(j_6) [\text{GeV}] >$	–		–		–		–		60	
$\Delta\phi(\text{jet}_i, E_T^{\text{miss}})_{\text{min}} >$	0.4 ($i = \{1, 2, (3 \text{ if } p_T(j_3) > 40 \text{ GeV})\}$)					0.4 ($i = \{1, 2, 3\}$), 0.2 ($p_T > 40 \text{ GeV jets}$)				
$E_T^{\text{miss}}/m_{\text{eff}}(Nj) >$	0.2	– ^a	0.3	0.4	0.25	0.25	0.2	0.15	0.2	0.25
$m_{\text{eff}}(\text{incl.}) [\text{GeV}] >$	1000	1600	1800	2200	1200	2200	1600	1000	1200	1500

(a) For SR A-medium the cut on $E_T^{\text{miss}}/m_{\text{eff}}(Nj)$ is replaced by a requirement $E_T^{\text{miss}}/\sqrt{H_T} > 15 \text{ GeV}^{1/2}$.

Figure 5: definition of signal regions in [4]

The cuts on m_{eff} can be motivated by following plots:

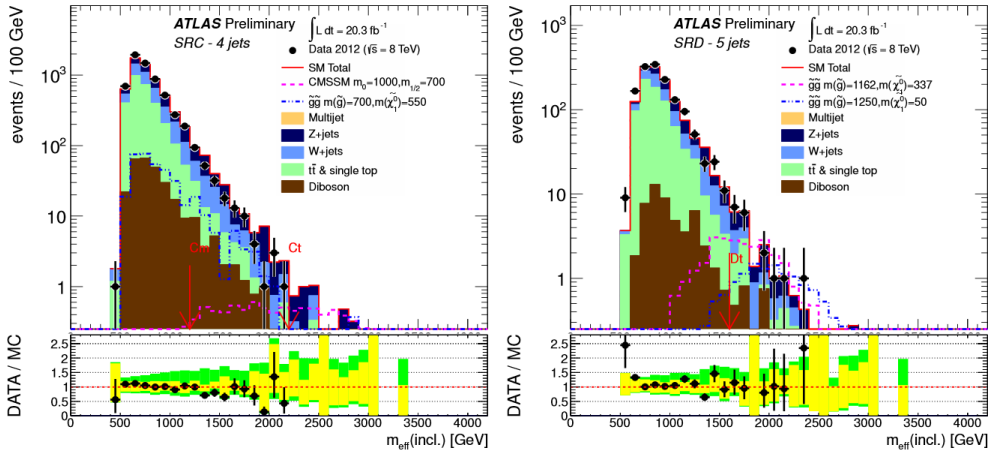


Figure 6: $m_{\text{eff}}(\text{incl.})$ distribution for SR C and D in [4], the red arrow denotes the cut

As one can see, the most of the signal shapes differ greatly from background shapes. The most important backgrounds were identified to be $Z \rightarrow \nu\nu + \text{jets}$, which was modelled by $\gamma + \text{jets}$ samples, multi-jets QCD events, $W \rightarrow \ell\nu + \text{jets}$ with misidentified leptons and $t\bar{t}$ and single- t backgrounds. The results can be seen in the following table:

Signal Region	A-loose	A-medium	B-medium	B-tight	C-medium	C-tight
MC expected events						
Diboson	428.6	15.0	4.3	0.0	25.5	0.0
Z/ γ^* +jets	2044.4	83.1	20.6	2.3	119.4	2.6
W+jets	2109.0	58.8	16.4	2.1	88.7	1.0
$t\bar{t}$ (+EW) + single top	785.9	8.2	2.0	0.3	45.9	0.3
Fitted background events						
Diboson	430 \pm 190	15 \pm 7	4.3 \pm 2.0	–	26 \pm 11	–
Z/ γ^* +jets	1870 \pm 320	57 \pm 11	16 \pm 5	0.2 \pm 0.5	80 \pm 29	0.0 ^{+0.6} _{-0.0}
W+jets	1540 \pm 260	42 \pm 11	10 \pm 4	1.6 \pm 1.2	55 \pm 18	0.7 \pm 0.9
$t\bar{t}$ (+EW) + single top	870 \pm 180	7.8 \pm 2.8	2.2 \pm 2.0	0.6 \pm 0.7	50 \pm 11	0.9 \pm 0.9
Multi-jets	33 \pm 33	–	0.1 \pm 0.1	–	–	–
Total bkg	4700 \pm 500	122 \pm 18	33 \pm 7	2.4 \pm 1.4	210 \pm 40	1.6 \pm 1.4
Observed	5333	135	29	4	228	0
$\langle \epsilon\sigma \rangle_{\text{obs}}^{95}$ [fb]	66.07	2.52	0.73	0.33	4.00	0.12
S_{obs}^{95}	1341.2	51.3	14.9	6.7	81.2	2.4
S_{exp}^{95}	1135.0 ^{+332.7} _{-291.5}	42.7 ^{+15.5} _{-11.4}	17.0 ^{+6.6} _{-4.6}	5.8 ^{+2.9} _{-1.8}	72.9 ^{+23.6} _{-18.0}	3.3 ^{+2.1} _{-1.2}
$p_0(Z_n)$	0.45 (0.1)	0.27 (0.6)	0.50 (0.0)	0.34 (0.4)	0.34 (0.4)	0.50 (0.0)

Figure 7: results of the analysis in [4]

Signal Region	D	E-loose	E-medium	E-tight
MC expected events				
Diboson	2.0	5.5	1.7	0.0
Z/ γ^* +jets	8.5	19.6	6.3	1.9
W+jets	4.8	23.1	5.2	0.8
$t\bar{t}$ (+EW) + single top	5.0	67.3	16.8	1.5
Fitted background events				
Diboson	2.0 \pm 2.0	5.5 \pm 2.1	1.7 \pm 0.8	–
Z/ γ^* +jets	3.8 \pm 2.5	12 \pm 7	2.9 \pm 2.6	0.4 \pm 0.6
W+jets	3.3 \pm 2.5	18 \pm 7	4.9 \pm 2.7	0.7 \pm 0.5
$t\bar{t}$ (+EW) + single top	5.8 \pm 2.1	76 \pm 19	20 \pm 6	1.7 \pm 1.4
Multi-jets	–	1.0 \pm 1.0	–	–
Total bkg	15 \pm 5	113 \pm 21	30 \pm 8	2.9 \pm 1.8
Observed	18	166	41	5
$\langle \epsilon\sigma \rangle_{\text{obs}}^{95}$ [fb]	0.77	4.55	1.41	0.41
S_{obs}^{95}	15.5	92.4	28.6	8.3
S_{exp}^{95}	13.6 ^{+5.1} _{-3.5}	57.3 ^{+20.0} _{-14.4}	21.4 ^{+7.6} _{-5.8}	6.5 ^{+3.0} _{-1.9}
$p_0(Z_n)$	0.32 (0.5)	0.03 (1.9)	0.14 (1.1)	0.22 (0.8)

Figure 8: results of the analysis in [4]

Since the number of observed events are consistent with the expected background events, exclusion limits can be set.

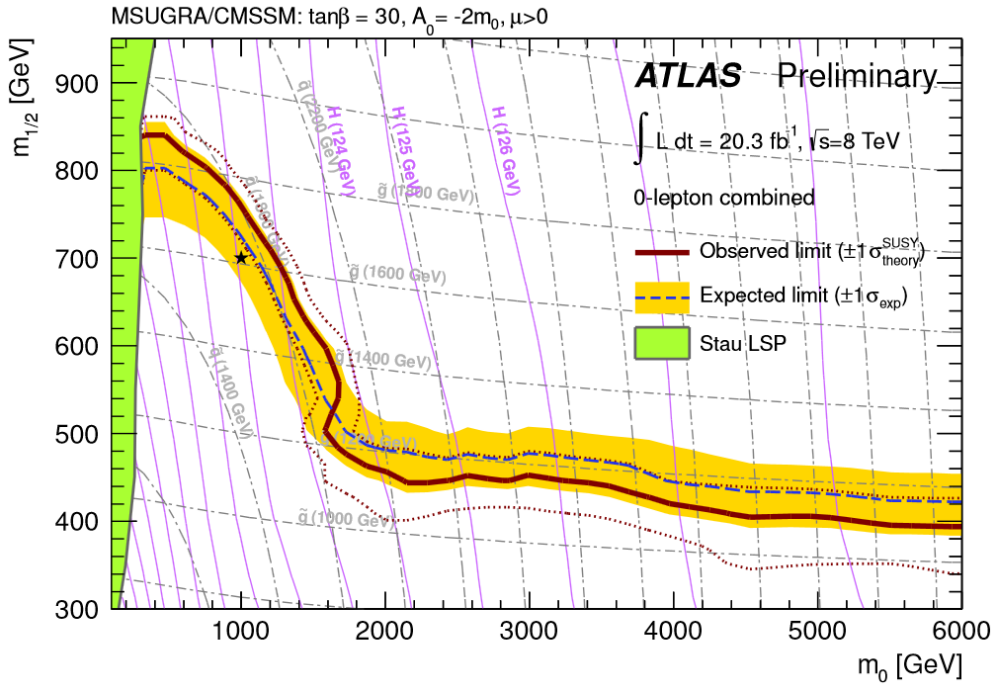


Figure 9: exclusion limits for the CMSSM of the analysis in [4]

For the cMSSM, gluino masses of around 1200 GeV and squark masses of around 1700 GeV can be excluded. For the different pMSSM decay scenarios gluino masses of around 1500 GeV can be excluded, while squark masses of up to 800 GeV, depending on the neutralino mass can be excluded.

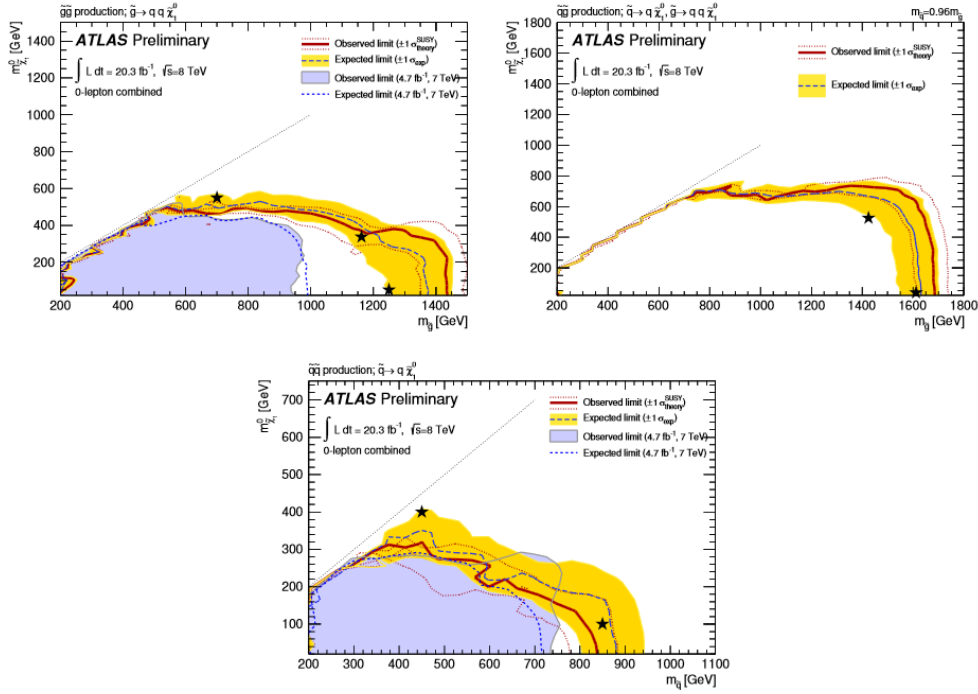


Figure 10: exclusion limits for three decay chain models of the analysis in [4]

4.2 2-6 jets + 1-2 leptons search by ATLAS

As seen before, many decays include leptons. In this search, additional isolated leptons are considered. One of the key problems is the definition of what leptons to call isolated. The lepton is only accepted, should it be either closer than $\Delta R = 0.2$ or further away than $\Delta R = 0.4$ from a jet. To obtain an isolated lepton in the first case, the jet will be ignored.

The decays analysed for the pMSSM-part look as follows:

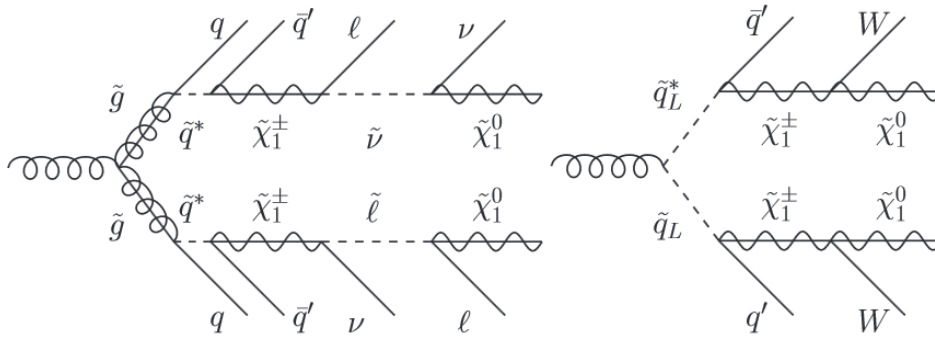


Figure 11: example for decays analysed in [5]

As one can see one expects the typical event shape as before, giving rise to similar signal regions as seen before:

	inclusive (binned) hard single-lepton		
	3-jet	5-jet	6-jet
N_ℓ	1 (electron or muon)		
p_T^ℓ (GeV)	> 25		
$p_{T, \text{add. } \ell}$ (GeV)	< 10		
N_{jet}	≥ 3	≥ 5	≥ 6
$p_{T, \text{jet}}^{\text{jet}}$ (GeV)	> 80, 80, 30	> 80, 50, 40, 40, 40	> 80, 50, 40, 40, 40, 40
$p_{T, \text{add. jets}}$ (GeV)	– (< 40)	– (< 40)	–
E_T^{miss} (GeV)	> 500 (300)	> 300	> 350 (250)
m_T (GeV)	> 150	> 200 (150)	> 150
$E_T^{\text{miss}}/m_{\text{eff}}^{\text{excl}}$	> 0.3	–	–
$m_{\text{eff}}^{\text{incl}}$ (GeV)	> 1400 (800)		> 600

Figure 12: example for definitions of signal regions in [5]

Which can again be motivated by a look at the distributions:

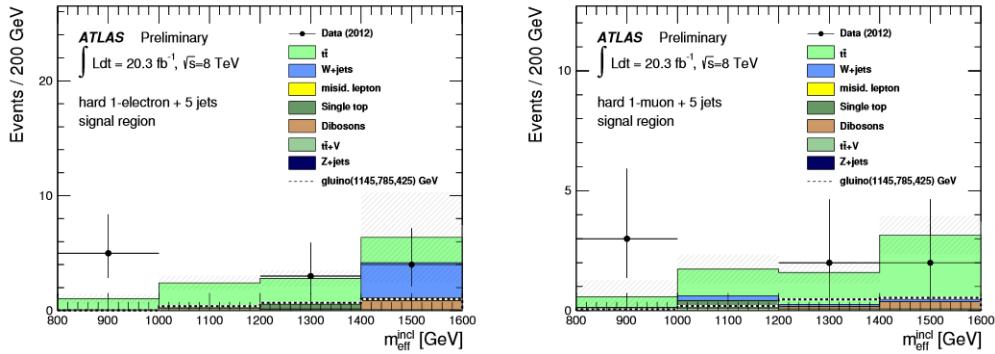


Figure 13: $m_{\text{eff}}^{\text{incl}}$ (incl.) distribution for SR hard 5 jets in [5]

The major backgrounds in this analysis consist of:

- $t\bar{t}$, reduced using a control region
- W +jets, reduced using a control region
- lepton misidentification, for example from $Z \rightarrow \nu\nu$ +jets
- single-top, dibosonic $t\bar{t} + W$ and $t\bar{t} + Z$ from theory

An example for the chosen control regions can be seen in the following overview

	soft single-lepton		soft dimuon
	3-jet	5-jet	2-jet
	W+jets / $t\bar{t}$		$t\bar{t}$
N_ℓ	1 (electron or muon)		2 (muons)
p_T^ℓ (GeV)	[10,25] (electron) , [6,25] (muon)		>25,6
$p_T^{\text{add. } \ell}$ (GeV)	< 7 (electron), < 6 (muon)		
$m_{\mu\mu}$ (GeV)	–	–	>15 and $ m_{\mu\mu} - m_Z > 10$
N_{jet}	[3,4]	≥ 5	≥ 2
$p_T^{\text{leading jet}}$ (GeV)	> 180		>70
$p_T^{\text{subleading jets}}$ (GeV)	> 25		
$N_{b\text{-tag}}$	0 / ≥ 1		≥ 1
E_T^{miss} (GeV)	[180,250]		> 170
m_T (GeV)	[40,80]		< 80
$\Delta R_{\text{min}}(\text{jet}, \ell)$	> 1.0	–	> 1.0

Figure 14: example for definitions of control regions for W+jets and $t\bar{t}$ in [5]

The total number of background events is fitted to data using Monte Carlo samples in this control region. Assuming a correct modelling of the shape, one can then transfer the result into the signal regions giving a number of expected events for that background. The estimated events are then compared with data:

Signal channel	$\langle \epsilon\sigma \rangle_{\text{obs}}^{95}$ [fb]	S_{obs}^{95}	S_{exp}^{95}	CL_B	$p(s=0)$
soft single-lepton one b -jet channels					
low-mass	0.43 (0.42)	8.8 (8.6)	$6.9^{+3.0}_{-2.0}$ ($6.9^{+3.4}_{-2.1}$)	0.76 (0.71)	0.26 (0.27)
high-mass	0.39 (0.38)	7.9 (7.7)	$6.3^{+1.9}_{-1.1}$ ($5.9^{+3.0}_{-1.9}$)	0.79 (0.75)	0.21 (0.22)
soft single-lepton two b -jet channels					
low-mass	0.66 (0.62)	13.4 (12.7)	$13.2^{+5.9}_{-4.1}$ ($13.1^{+5.6}_{-3.8}$)	0.52 (0.46)	0.50 (0.50)
high-mass	0.26 (0.24)	5.3 (4.9)	$5.3^{+2.4}_{-1.4}$ ($5.5^{+2.8}_{-1.8}$)	0.50 (0.40)	0.50 (0.50)
soft single-lepton channels					
3-jet	0.40 (0.39)	8.1 (8.1)	$7.3^{+2.7}_{-1.8}$ ($6.8^{+3.3}_{-2.1}$)	0.67 (0.66)	0.36 (0.31)
5-jet	0.35 (0.33)	7.1 (6.8)	$10.0^{+3.6}_{-3.0}$ ($9.8^{+4.2}_{-2.9}$)	0.15 (0.15)	0.50 (0.50)
soft dimuon channel	0.57 (0.54)	11.5 (11.1)	$5.9^{+2.1}_{-1.0}$ ($6.5^{+3.1}_{-1.9}$)	0.98 (0.92)	0.01 (0.02)
binned hard single-lepton channels					
3-jet (electron)	0.97 (0.98)	19.8 (19.9)	$20.2^{+8.3}_{-4.8}$ ($20.7^{+7.9}_{-5.6}$)	0.47 (0.45)	0.50 (0.50)
3-jet (muon)	0.57 (0.52)	11.6 (10.6)	$15.6^{+5.8}_{-3.8}$ ($15.8^{+6.5}_{-4.4}$)	0.13 (0.12)	0.50 (0.50)
5-jet (electron)	0.63 (0.60)	12.7 (12.1)	$12.6^{+3.2}_{-2.7}$ ($12.2^{+4.5}_{-3.2}$)	0.50 (0.49)	0.50 (0.50)
5-jet (muon)	0.38 (0.36)	7.7 (7.2)	$7.6^{+2.8}_{-2.4}$ ($7.3^{+3.4}_{-2.2}$)	0.53 (0.49)	0.50 (0.50)
6-jet (electron)	0.33 (0.34)	6.6 (6.8)	$7.8^{+3.1}_{-2.4}$ ($7.7^{+3.6}_{-2.4}$)	0.32 (0.37)	0.50 (0.50)
6-jet (muon)	0.35 (0.35)	7.1 (7.1)	$7.1^{+3.4}_{-1.4}$ ($7.4^{+3.5}_{-2.3}$)	0.50 (0.46)	0.50 (0.50)
inclusive hard single-lepton channels					
3-jet (electron)	0.30 (0.28)	6.0 (5.7)	$5.7^{+2.2}_{-1.5}$ ($5.6^{+2.9}_{-1.8}$)	0.56 (0.51)	0.48 (0.48)
3-jet (muon)	0.38 (0.37)	7.7 (7.5)	$5.1^{+2.0}_{-1.5}$ ($5.1^{+2.7}_{-1.7}$)	0.89 (0.82)	0.13 (0.13)
5-jet (electron)	0.30 (0.29)	6.0 (5.9)	$5.4^{+2.3}_{-1.5}$ ($5.5^{+2.9}_{-1.7}$)	0.60 (0.56)	0.43 (0.43)
5-jet (muon)	0.22 (0.21)	4.6 (4.2)	$4.7^{+1.9}_{-1.2}$ ($4.7^{+2.5}_{-1.6}$)	0.44 (0.41)	0.50 (0.50)
6-jet (electron)	0.23 (0.22)	4.6 (4.4)	$4.4^{+1.9}_{-0.8}$ ($4.4^{+2.5}_{-1.5}$)	0.56 (0.49)	0.50 (0.50)
6-jet (muon)	0.15 (0.12)	3.0 (2.5)	$4.1^{+1.3}_{-1.1}$ ($3.8^{+2.3}_{-1.3}$)	0.13 (0.16)	0.50 (0.50)

Figure 15: results of the analysis in [5]

Again, the data is in very good agreement with the SM, leading to exclusion limits for SUSY scenarios:

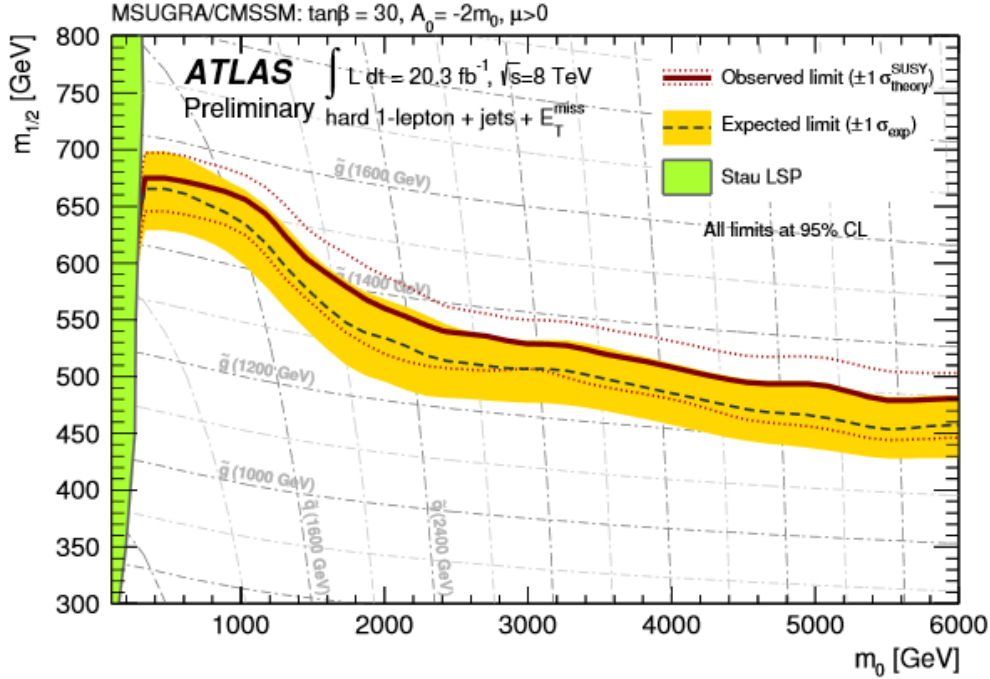


Figure 16: exclusion limits for the CMSSM of the analysis in [5]

For the cMSSM gluino masses of about 1100 GeV can be excluded, while for the pMSSM gluino masses of around 1200 GeV for neutralinos of about 500 GeV can be excluded.

4.3 Search using the variable α_T and b-quark multiplicity by CMS

This search introduces a variable called α_T as discriminant:

$$\alpha_T = \frac{E_T^{j2}}{M_T}$$

$$M_T = \sqrt{(E_T^{j1} + E_T^{j2})^2 - (p_x^{j1} + p_x^{j2})^2 - (p_y^{j1} + p_y^{j2})^2}$$

$$H_T = \sum_{i=1}^{n_{\text{jet}}} E_T^i$$

$$\mathcal{H}_T = \left| \sum_{i=1}^{n_{\text{jet}}} p_T^i \right|$$

Using this definition, however, α_T can only be used for events with 2 jets. To generalize this definition, all jets are summed up in pair such that their H_T values are as close together as possible. Using ΔH_T as difference between the H_T of the pairs one obtains:

$$\alpha_T = \frac{H_T - \delta H_T}{2\sqrt{H_T^2 - \mathcal{H}_T^2}}$$

This analysis is tailored towards special decay chains modelled by separate Monte Carlo samples:

Model	Production/decay mode	Reference model	
		m_{parent} [GeV]	m_{LSP} [GeV]
D1	$pp \rightarrow \tilde{q}\tilde{q}^* \rightarrow q\tilde{\chi}_1^0 \bar{q}\tilde{\chi}_1^0$	600	250
D2	$pp \rightarrow \tilde{b}\tilde{b}^* \rightarrow b\tilde{\chi}_1^0 \bar{b}\tilde{\chi}_1^0$	500	150
D3	$pp \rightarrow \tilde{t}\tilde{t}^* \rightarrow t\tilde{\chi}_1^0 \bar{t}\tilde{\chi}_1^0$	400	0
G1	$pp \rightarrow \tilde{g}\tilde{g} \rightarrow q\bar{q}\tilde{\chi}_1^0 q\bar{q}\tilde{\chi}_1^0$	700	300
G2	$pp \rightarrow \tilde{g}\tilde{g} \rightarrow b\bar{b}\tilde{\chi}_1^0 b\bar{b}\tilde{\chi}_1^0$	900	500
G3	$pp \rightarrow \tilde{g}\tilde{g} \rightarrow t\bar{t}\tilde{\chi}_1^0 t\bar{t}\tilde{\chi}_1^0$	850	250

Figure 17: definition of signal decays in [6]

The signal regions are defined as follows:

Analysis bin H_T [GeV]	Trigger thresholds		Trigger efficiency [%]	
	H_T [GeV]	α_T	$2 \leq n_{\text{jet}} \leq 3$	$n_{\text{jet}} \geq 4$
275–325	250	0.55	$89.1^{+0.4}_{-0.4}$	$83.7^{+0.6}_{-0.6}$
325–375	300	0.53	$98.7^{+0.2}_{-0.3}$	$98.2^{+0.4}_{-0.5}$
375–475	350	0.52	$99.0^{+0.4}_{-0.5}$	$99.7^{+0.2}_{-0.6}$
≥ 475	400	0.51	$100.0^{+0.0}_{-0.6}$	$100.0^{+0.0}_{-0.8}$

Figure 18: definition of signal regions in [6]

Decay chains and signal regions are connected by following table:

Model	n_{jet}	n_b
D1	2–3	0
D2	2–3	1, 2
D3	≥ 4	1, 2
G1	≥ 4	0
G2	≥ 4	2, 3, ≥ 4
G3	≥ 4	2, 3, ≥ 4

Figure 19: Channels used for exclusion by model [6]

for different b multiplicities, different backgrounds are relevant:

- Z +jets and W +jets for $n_b = 0$
- $t\bar{t}$ and single-top for $n_b \geq 1$

While the usually important QCD multijet background is suppressed by cuts, the results of the analysis are again in agreement with the SM:

		H_T bin [GeV]								
n_{jet}	n_b	275–325	325–375	375–475	475–575	575–675	675–775	775–875	875– ∞	
SM	2–3	0	6235 ⁺¹⁰⁰ ₋₆₇	2900 ⁺⁶⁰ ₋₅₄	1955 ⁺³⁴ ₋₃₉	558 ⁺¹⁴ ₋₁₅	186 ⁺¹¹ ₋₁₀	51.3 ^{+3.4} _{-3.8}	21.2 ^{+2.3} _{-2.2}	16.1 ^{+1.7} _{-1.7}
Data	2–3	0	6232	2904	1965	552	177	58	16	25
SM	2–3	1	1162 ⁺³⁷ ₋₂₉	481 ⁺¹⁸ ₋₁₉	341 ⁺¹⁵ ₋₁₆	86.7 ^{+4.2} _{-5.6}	24.8 ^{+2.8} _{-2.7}	7.2 ^{+1.1} _{-1.0}	3.3 ^{+0.7} _{-0.7}	2.1 ^{+0.5} _{-0.5}
Data	2–3	1	1164	473	329	95	23	8	4	1
SM	2–3	2	224 ⁺¹⁵ ₋₁₄	98.2 ^{+8.4} _{-6.4}	59.0 ^{+5.2} _{-6.0}	12.8 ^{+1.6} _{-1.6}	3.0 ^{+0.9} _{-0.7}	0.5 ^{+0.2} _{-0.2}	0.1 ^{+0.1} _{-0.1}	0.1 ^{+0.1} _{-0.1}
Data	2–3	2	222	107	58	12	5	1	0	0
SM	≥ 4	0	1010 ⁺³⁴ ₋₂₄	447 ⁺¹⁹ ₋₁₆	390 ⁺¹⁹ ₋₁₅	250 ⁺¹² ₋₁₁	111 ⁺⁹ ₋₇	53.3 ^{+4.3} _{-4.3}	18.5 ^{+2.4} _{-2.4}	19.4 ^{+2.5} _{-2.7}
Data	≥ 4	0	1009	452	375	274	113	56	16	27
SM	≥ 4	1	521 ⁺²⁵ ₋₁₇	232 ⁺¹⁵ ₋₁₂	188 ⁺¹² ₋₁₁	106 ⁺⁶ ₋₆	42.1 ^{+4.1} _{-4.4}	17.9 ^{+2.2} _{-2.0}	9.8 ^{+1.5} _{-1.4}	6.8 ^{+1.2} _{-1.1}
Data	≥ 4	1	515	236	204	92	51	13	13	6
SM	≥ 4	2	208 ⁺¹⁷ ₋₉	103 ⁺⁹ ₋₇	85.9 ^{+7.2} _{-6.9}	51.7 ^{+4.6} _{-4.7}	19.9 ^{+3.4} _{-3.0}	6.8 ^{+1.2} _{-1.3}	1.7 ^{+0.7} _{-0.4}	1.3 ^{+0.4} _{-0.3}
Data	≥ 4	2	204	107	84	59	24	5	1	2
SM	≥ 4	3	25.3 ^{+5.0} _{-4.2}	11.7 ^{+1.7} _{-1.8}	6.7 ^{+1.4} _{-1.2}	3.9 ^{+0.8} _{-0.8}	2.3 ^{+0.6} _{-0.6}	1.2 ^{+0.3} _{-0.4}	0.3 ^{+0.2} _{-0.1}	0.1 ^{+0.1} _{-0.1}
Data	≥ 4	3	25	13	4	2	2	3	0	0
SM	≥ 4	≥ 4	0.9 ^{+0.4} _{-0.7}	0.3 ^{+0.2} _{-0.2}	0.6 ^{+0.3} _{-0.3}	–	–	–	–	–
Data	≥ 4	≥ 4	1	0	2	–	–	–	–	–

Figure 20: Confrontation of SM and data in [6]

This again gives rise to exclusion limits. Each decay chain is given a channel in the analysis, resulting in following exclusions:

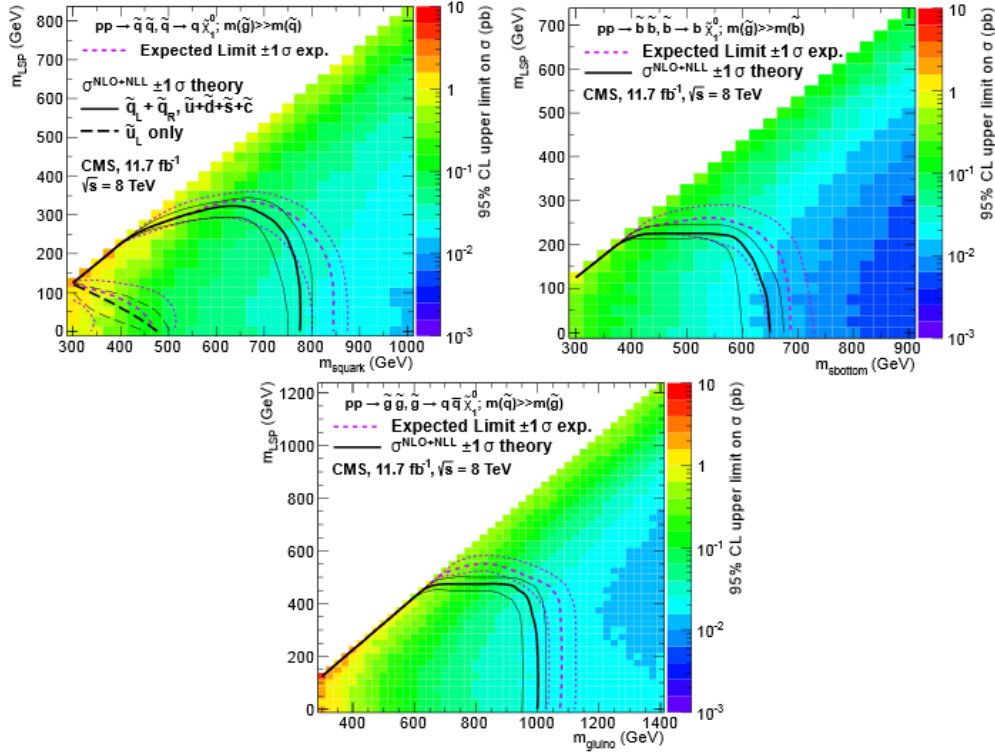


Figure 21: exclusion limits for three of the decay chains of the analysis in [6]

The different chains give different limits on the gluino mass of up to 1000 GeV for neutralino masses of up to 400 GeV and squark masses of 780 GeV for a neutralino of 200 GeV. Also, one can give limits on the stop mass of about 450 GeV using the total production cross section.

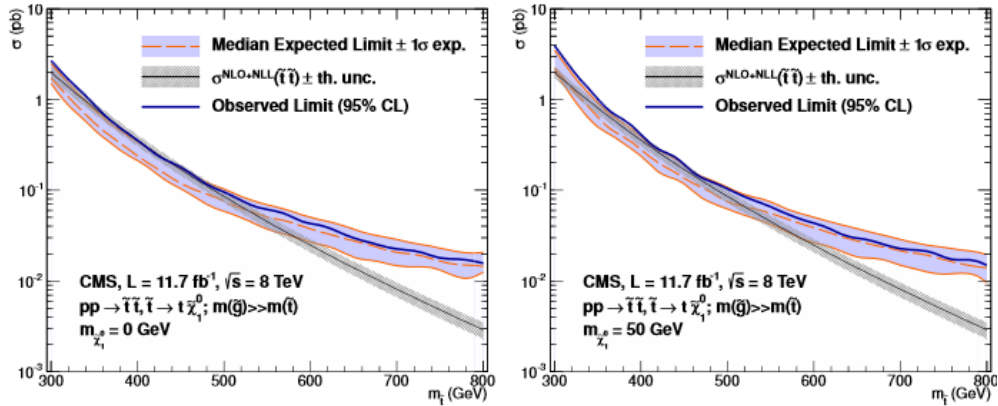


Figure 22: exclusion limits for the production cross section of stop pairs given in [6]

References

- [1] Fehling-Kaschek, M.: Search for Scalar Bottom and Top Quarks with the ATLAS Detector at the LHC, dissertation, Uni Freiburg, 2013
- [2] Jakobs, K.: Searches for Physics Beyond the Standard Model at the LHC, talk, Les Houches, 2011
- [3] Jakobs, K.: Search for Supersymmetry at the LHC, talk, Les Houches, 2011
- [4] ATLAS Collaboration: ATLAS-CONF-2013-047, note, 2013
- [5] ATLAS Collaboration: ATLAS-CONF-2013-062, note, 2013
- [6] CMS Collaboration: CMS-SUS-12-028, paper, 2013
- [7] Ellis, J: BEYOND THE STANDARD MODEL FOR HILLWALKERS, lecture, 1998